Sedimentological and glaciotectonic interpretation of georadar data from the margin of the Vig ice-push ridge, NW Sjælland, Denmark

Cecilie Skovsø Andersen and Peter Roll Jakobsen

Glaciotectonic deformations often result in a high degree of variability, including glaciotectonic and sedimentary variability. Redeposition of sediments during deformation increases the variability. Ground-penetrating radar (GPR) has proven to be a good method to determine sedimentary structures in glaciofluvial deposits (Olsen & Andreasen 1994; Van Overmeeren 1998) as well as glaciotectonic structures (Busby & Merrit 1999; Overgaard & Jakobsen 2001). Reflection facies analysis (radar facies) is a useful tool in the characterisation and interpretation of deformed sediments (Van Overmeeren 1998; Jakobsen & Overgaard 2002; Lerche *et al.* 2014).

A GPR survey was carried out at Jyderup Skov in Odsherred in north-west Sjælland (Fig. 1). The presence of parallel ridges in the area indicates glaciotectonic deformation. The aim of the GPR study was to map the interior of the ridge complex and to interpret the genesis of the ridges.

Geological setting

The morphology of Odsherred in the north-western part of Sjælland is dominated by three large arc-shaped ice-push ridges (Fig. 1A). The ice-push ridges (arcs) were formed in the Late Weichselian during the Bælthav readvance and glaciofluvial deposits related to the ridge formation have been dated to be *c.* 17 000 years (Houmark-Nielsen 2008). The arcs cut each other and they were formed by three ice readvances of ice-lobes situated east of them. Each arc is a polymorphological landscape built-up of several landscape types. Data from boreholes show that the arcs contain dislocated Paleocene clay and Weichselian marine deposits indicating that the interior of the arcs is affected by glaciotectonic deformation. The investigated area is located in the western part of the Vig arc (Fig. 1B), which is situated in the centre of three arcs in Odsherred with the reclaimed Sidinge Fjord to the east forming a central depression. On the stoss side towards Sidinge Fjord is a terrain of smooth ground moraine. The upper part of the Vig arc is characterised by hummocky moraine and the western part consists of elongated ice-marginal moraines. Larger flat-topped kames occur within the hummocky moraine landscape and west of the ice-marginal moraine glaciofluvial deposits form an outwash plain. A number of elongated parallel ridges occur in the eastern part of the outwash plain (Fig. 1C). A raw-material investigation shows that at least the upper 10 m consist of sand and gravel (Region Sjælland 2011), and borehole information shows the presence of sandy till.

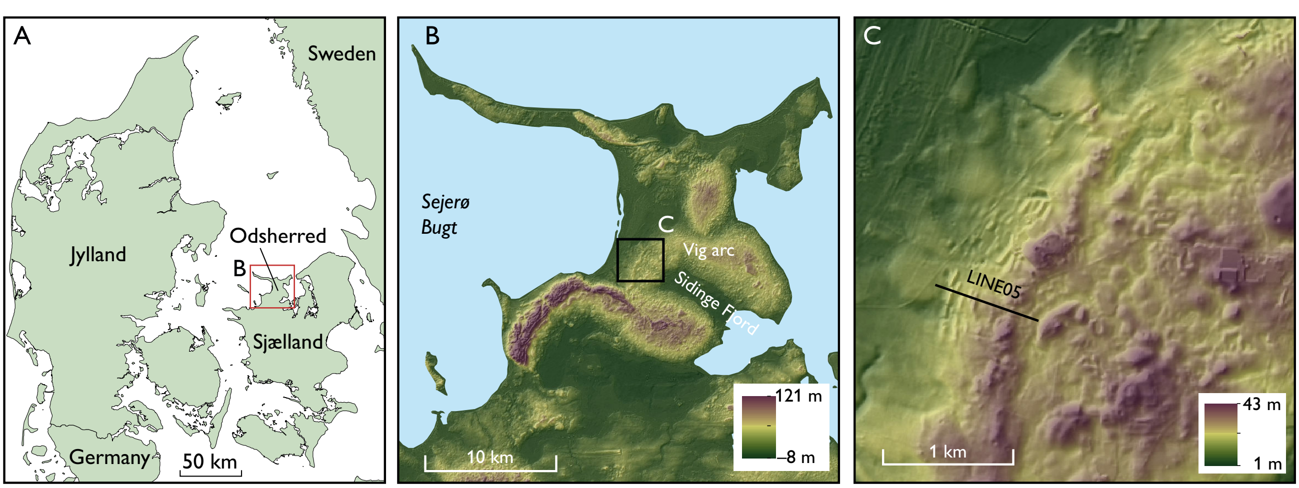

Fig. 1. **A**: Map of Denmark showing the location of Odsherred. **B**: Terrain model of Odsherred, NW Sjælland, with index map. **C**: Terrain model of the investigated area showing the location of the georadar line LINE05 over the ice-margin ridges.

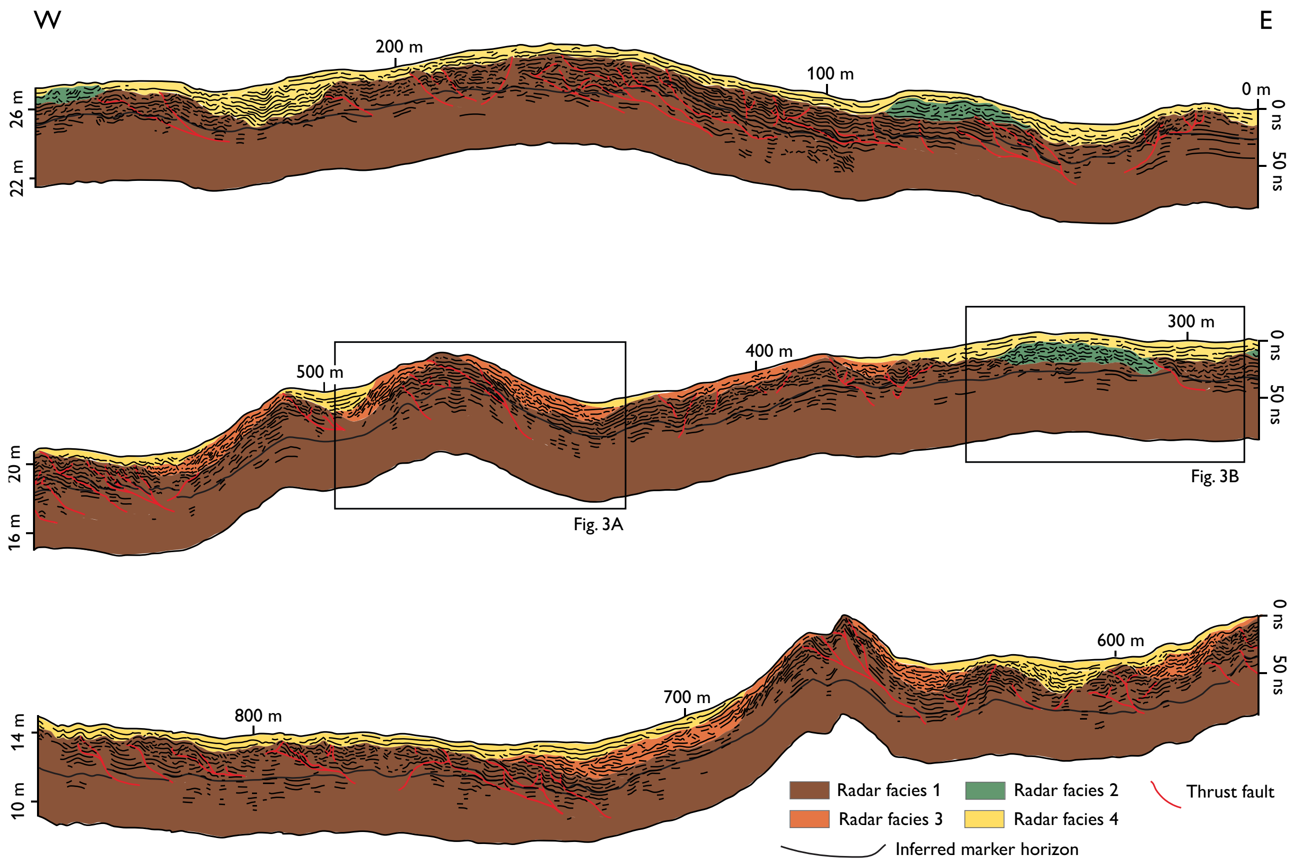

Fig. 2. Interpretation of the ground-penetrating radar profile LINE05. The scale to the left shows metres above sealevel. The scale to the right shows two-way travel time in nanoseconds. The black line is an inferred marker horizon used for structural analysis. The vertical exaggeration is 1:4. The black boxes indicate details shown in Fig. 3.

Georadar survey and processing parameters

Five GPR lines were made perpendicular to the ridges and one was recorded parallel to the overall strike of the ridges. The occurrence of forest roads and paths in Jyderup Skov determined the location of the lines. The data were acquired in October 2015 using a 250 MHz Sensors & Software Inc. georadar. Due to the forest setting shielded antennae on a skid plate were used with a *c.* 40 cm offset. The traces were sampled with a step size of *c.* 5 cm and then stacked by a factor of 8.

The line LINE05 provides the best image of the internal structure of the ridges (Figs 1B, 2). Processing of the raw LINE05 was carried out using PulseEKKO software by Sensors & Software Inc. in the following steps: first, a Dewow filter with an operational length of 1 pulse width was applied, followed by a Stolt migration with an estimated velocity of 0.133 mns^{-1}, which is typical value for dry sand. An automatic gain control with a pulse width of 1 and a maximum scaling factor of 700 was then applied, before the final topographic corrections were added. The vertical resolution is *c.* 20 cm.

Georadar facies description and interpretation

The LINE05 profile is 850 m long and cross-cuts 10 ridges excluding the moraine and the two ridges behind the ice-marginal moraine of the Vig arc (Fig. 2). Four radar facies are distinguished in the profile.

Radar facies 1 (Fig. 2) is interpreted as glaciofluvial sand and gravel based on the relatively strong parallel to subparallel reflections with high contrast, which are moderately continuous to discontinuous. Borehole data indicate that glaciofluvial sand and gravel are found to a depth of *c.* 20 m below the terrain surface. The reflections are primarily planar to wavy shaped, but antiforms and synforms are also found (8.5 m wide on average; Figs 2, 3A). The antiforms have a slightly asymmetric appearance with the western flank being steeper (typically *c.* 12°) than the eastern flank (typically *c.* 6°). The antiform has an interlimb angle of typically *c.* 160°. The reflectors show frequent displacements, which we interpret as thrust faults (Figs 2, 3A). The offset is between 0.20 m and 4.80 m with an average of 1.36 m. The reflections dip 4.0° to 13.6° dominantly to the east and are generally steepening upwards in a gentle concave to steep convex dipping pattern. The facies is truncated by facies 2, 3 and 4 in a concordant and erosional way (Fig. 2). We describe the detailed characteristics of the thrusts in the next section.

In radar facies 2 (Figs 2, 3B) the reflections are discontinuous and show a relatively low amplitude contrast. The reflection pattern is chaotic at *c.* 280 m to subparallel at *c.* 325 m (Fig. 3B) and *c.* 75 m, where the reflections dip downwards at the ends of the facies. Based on the facies characteristics, this facies is interpreted as a gravelly ablation till. Facies 2 is found in patches and it drapes facies 1.

Radar facies 3 (Figs 2, 3A) consists of steepening upward (on average 10°) moderately continuous to discontinuous and subparallel reflections, this facies is mainly found on the western slope of the ridges. The reflection pattern is similar to facies 1. Based on the position of the facies and the reflection pattern, facies 1 is likely to be the source of the sediments of facies 3 that were redeposited as solifluction sediments. This interpretation is in good agreement with the primary location of the facies on the western flank of the ridges, where it is more inclined to slope failure.

In radar facies 4 (Fig. 2) the reflection pattern can be described as continuous, parallel and diverging with a high density of downlaps and onlaps in the crests between ridges. The facies drapes the other three facies, and in some areas, it truncates facies 1 in an erosional way. Facies 4 has a strong relative amplitude contrast. Based on the reflection pattern, facies 4 is interpreted as sand and gravel. The facies is typically thin and lacking on top of some of the ridges (Figs 2, 3A). However, it is locally thick on the crests. The facies is interpreted as post-deformation deposits.

Structural geology

The thrust-fault planes are commonly concave and convex rotating listric faults steepening upwards following and cross-cutting the bedding, with a dip of 2.5° to 21.9° (13.4° on average) mainly to the east. The westward dipping thrust faults are usually small and often back-thrusts from the more extensive eastward dipping thrusts. Some of the thrusts are clustered in a complex splay pattern, where the main thrust jacks up with each splaying thrust. These thrust faults are interpreted as linked contractional, leading imbricate stacks, originating from the same root at a detachment. The displacement is greatest at the frontal thrust sheet. The leading imbricate stacks are primarily located beneath the ridges on the eastern flank, but they also occur on the western flanks in association with antiforms and synforms. Fault-bend-folding style of thrusting with hanging-wall ramp-flat-ramps and footwall flat-ramp-flats is evident from the concave–convex shape of the bedding along the fault plane. Fault propagation folding is seen in the imbricate stacks where the tip line terminates in the bedding. By drawing an inferred marker horizon (Fig. 2) on LINE05, the shortening of the line, caused by thrusting and folding, is calculated to be 12% of its initial length before deformation.

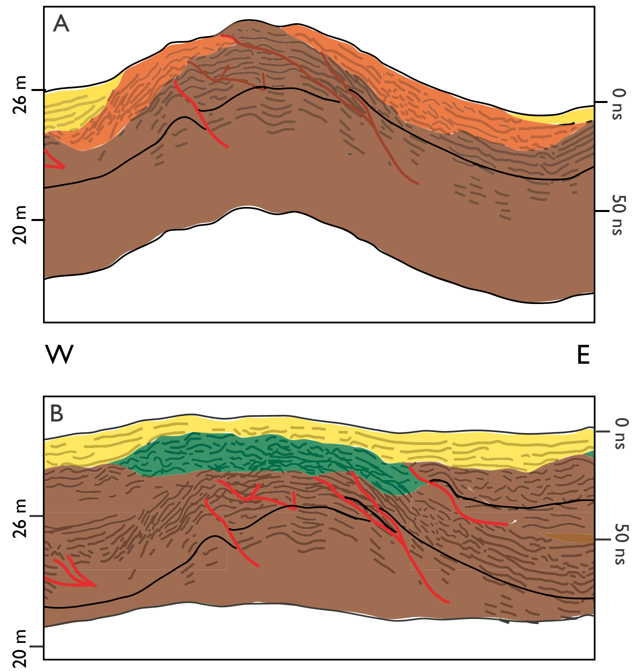

Fig. 3. Details from Fig. 2 (same legend as Fig. 2). **A**: Ridge formed by thrusting, and subsequently smoothened by radar facies 3 and 4. **B**: Relationship between radar facies 1, 2 and 4.

Formation of the ridges

The formation of the ridges can be described tectono-stratigraphically in three steps:

Pre-tectonic deposits: Radar facies 1 was deposited as glaciofluvial sand and gravel on a pro-glacial outwash plain. During a syn- and post-depositional event, radar facies 1 was folded and thrust into gentle anti- and synforms. The thrusts are dense on the eastern flank of the antiforms, and occur as thick, wide, complex imbricate fans. The slight asymmetry of the anti- and synforms and the dip direction of the thrusts and bedding indicate a direction of primary deformational stress from the east.

Tectonically penecontemporaneous deposits: Radar facies 2 was deposited penecontemporanously as an ablation till. It occurs in patches and is only seen in one borehole (DGU no 190.196) *c.* 250 m south-west of LINE05, where the upper 2 m consist of sandy and gravelly till. Radar facies 2 is recognised in three places along LINE05, at *c.* 75 m, *c.* 280 m and *c.* 325 m. At *c.* 325 m, the radar section cuts an elevated area, which does not have the distinct ridge morphology seen elsewhere. The flattened morphology is in good agreement with deposition of ablation till, in contrast to the deformed elongated ridges elsewhere in the area. At *c.* 75 m the radar section is within an area of former stagnant ice, where ablation till should be expected.

Post-tectonic deposition: After the deformation came to an end, erosion of radar facies 1 occurred, and some thrust sheets are clearly truncated by solifluction sediments (radar facies 3) and post-deformation deposits (radar facies 4).

The small parallel ridges west of the large Vig arc may have been formed in a single deformational event creating a thin-skinned thrust-fault complex in a gravity-spreading environment (Jakobsen & Overgaard 2002; Pedersen 2005) or as annual moraines formed at an oscillating ice-margin (Krüger 1995; Benediktsson *et al.* 2009). The presence of till deposits within the area with the small ridges indicates that the ice margin was situated in the area. The topographic relief of the ridges is pronounced and there is no indication of erosion of the top of the ridges. Thus, the glacier has not moved past the individual ridges. We therefore suggest that the ridges were formed as ice-marginal push moraines created by seasonal advances and retreats of the ice margin.

Conclusions

Ground-penetrating radar was used to map the sedimentological and glaciotectonic structures of a series of parallel morine ridges of an area west of the Vig arc in Odsherred. The GPR profiles have a high resolution that allows detailed sedimentological and structural analyses. Four radar facies are distinguished which represent different sedimentary environments and degrees of deformation and three tectonostratigraphic sequences are recognised: pre-tectonic, tectonically penecontemporaneous and post-tectonic deposits.

The interior of the ridges is characterised by thrust faults and folds created by deformation from the east and the ridge morphology is clearly associated with the deformation structures. Subsequently the ridge morphology has been smoothened by post-tectonic sedimentation. We suggest that ridges seen on the proximal part of the outwash plain, west of the Vig arc, were formed as ice-push moraines by seasonal advances and retreats of the ice margin.

References

Benediktsson, Í.Ö., Ingólfsson, Ó., Schomacker, A. & Kjær, K.H. 2009: Formation of submarginal and proglacial end moraines: implications of ice-flow mechanism during the 1963-64 surge of Brúarjökull, Iceland. Boreas **38**, 440–457.

Busby, J.P. & Merrit, J.W. 1999: Quaternary deformation mapping with ground penetrating radar. Journal of Applied Geophysiscs **41**, 75–91.

Houmark-Nielsen, M. 2008: Testing OSL failures against a regional Weichselian glaciation chronology from southern Scandinavia. Boreas **37**, 660–677.

Jakobsen, P.R. & Overgaard, T. 2002: Georadar facies and glaciotectonic structures in ice marginal deposits northwest Zealand, Denmark. Quarternary Science Reviews **21**, 917–927.

Krüger, J. 1995: Origin, chronology and climatological significance of annual-moraine ridges at Myrdaljökull, Iceland. The Holocene **5**, 420–427.

Lerche, H., Jakobsen, P.R. & Pedersen, S.A.S. 2014: Ribbed moraines formed during the retreat of the Scandinavian ice sheet from eastern Himmerland, NE Jylland, Denmark. Geological Survey of Denmark and Greenland Bulletin **31**, 39–42.

Pedersen, S.A.S. 2005: Structural analysis of the Rubjerg Knude Glaciotectonic Complex, Vendsyssel, northern Denmark. Geological Survey of Denmark and Greenland Bulletin **8**, 192 pp.

Olsen, H. & Andreasen, F. 1994: Sedimentology and ground-penetrating radar characteristics of a Pleistocene sandur deposit. Sedimentary Geology **99**, 1–15.

Overgaard, T. & Jakobsen, P.R. 2001: Mapping of glaciotectonic deformation in an ice marginal environment with ground penetrating radar. Journal of Applied Geophysics **47**, 191–197.

Region Sjælland 2011: Råstofkortlægning. Rapport **8**, sand, grus, sten, Jyderup, Odsherred Kommune, 38 pp. *http://jupiter.geus.dk/Rapportdb/Grundvandsrapport.seam?grundvandsrapportRapportid=90959*

Van Overmeeren, R.A. 1998: Radar facies of unconsolidated sediments in the Netherlands: A radar stratigraphic interpretation method for hydrogeology. Journal of Applied Geophysics **40**, 1–18.

Authors' addresses

C.S.A., *Orbicon, Linnés Alle 2, 2630 Taastrup*, E-mail: *cesa@orbicon.dk.*

P.R.J., *Geological Survey of Denmark and Greenland, Øster Voldgade 10, DK-1350 Copenhagen K, Denmark.*